

Silicon Carbonitride Thin-Film Coatings Fabricated by Remote Hydrogen–Nitrogen Microwave Plasma Chemical Vapor Deposition from a Single-Source Precursor: Growth Process, Structure, and Properties of the Coatings

A. M. Wrobel, I. Blaszczyk-Lezak, A. Walkiewicz-Pietrzykowska

Centre of Molecular and Macromolecular Studies, Polish Academy of Sciences,
Sienkiewicza 112, PL-90-363 Lodz, Poland

Received 15 March 2005; accepted 19 June 2006

DOI 10.1002/app.26109

Published online in Wiley InterScience (www.interscience.wiley.com).

ABSTRACT: Silicon carbonitride (Si:C:N) films were produced by remote hydrogen–nitrogen microwave plasma chemical vapor deposition (RP-CVD) from a 1,1,3,3-tetra-methylsilylazane precursor with a nitrogen content $\{[N_2]/([H_2] + [N_2])\}$ of 0.88 in the plasma-generating mixture and a substrate temperature in the range of 30–400°C. The effects of the substrate temperature on the rate and yield of the RP-CVD process and chemical structure (examined by Fourier transform infrared spectroscopy) of the result-

ing films were investigated. The Si:C:N film properties were characterized in terms of the density, hardness, elastic modulus, and friction coefficient. With the IR structural data, reasonable structure–property relationships were determined. © 2007 Wiley Periodicals, Inc. *J Appl Polym Sci* 105: 122–129, 2007

Key words: films; infrared spectroscopy; mechanical properties; structure-property relations

INTRODUCTION

Silicon carbonitride (Si:C:N) thin-film coatings, because of their superior useful properties, have recently attracted great interest. These materials exhibit high hardness,^{1–12} a low friction coefficient,^{8,10} good wear resistance,¹² strong adhesion to a substrate,^{9,12} a wide optical band gap,^{1,13–15} good field emission characteristics,^{16–18} low electrical conductivity,^{14,15} and outstanding high-temperature oxidation resistance.¹⁹ In view of their unique properties, Si : C : N films are very promising coatings for a wide range of technological applications. Si : C : N is considered to be a serious rival for other superhard materials, such as cubic boron nitride.²⁰

Of the various methods used for the production of Si:C:N films, chemical vapor deposition (CVD) from a variety of organosilicon compounds as single-source precursors appears to be very effective. These techniques include the fabrication of Si:C:N films by thermal CVD from ethylcyclosilazanes,²¹ Ar-ion-beam-induced

CVD from hexamethyldisilazane,²² direct plasma chemical vapor deposition (DP-CVD) from hexamethyldisilazane,^{1,6,9,12} bis(trimethylsilyl)carbodiimide,¹² and bis(dimethylamino)dimethylsilane,²³ as well as remote hydrogen–nitrogen microwave plasma chemical vapor deposition (RP-CVD) from 1-dimethylsilyl-2,2-dimethylhydrazine,²⁴ dimethylbis(2,2-dimethylhydrazino)silane,²⁴ hexamethyldisilazane,^{25–28} 1,1,3,3-tetra-methylsilylazane (TMDSN),^{29,30} (dimethylamino)dimethylsilane,³¹ and tris(dimethylamino) silane.³²

The last technique (RP-CVD) is particularly important for the fabrication of high-quality, defect-free coatings for advanced technology because it offers well-controlled growth conditions free of damaging effects arising from charged-particle bombardment or high-energy ultraviolet irradiation.^{29–31} In this work, we report on the fabrication of Si:C:N thin-film coatings by RP-CVD with TMDSN $[(Me_2HSi)_2NH]$ as a single-source precursor and a hydrogen–nitrogen mixture as a plasma-generating upstream gas. The results of our previous study of this process revealed a strong effect of the nitrogen content in the plasma-generating mixture (H_2-N_2) on the Si : C : N film growth rate and deposition yield, resulting from the contribution of hydronitrene (NH), a highly reactive coreagent produced in the plasma and fed into the CVD reactor.²⁹ A maximum in the growth rate and deposition yield found for the nitrogen content $\{c_N = [N_2]/([H_2] + [N_2])\}$ of 0.88 corresponded to the maximum content of the NH species in the reactor determined by the opti-

This article is dedicated to the memory of Professor Marian Kryszewski.

Correspondence to: A. M. Wrobel (amwrobel@cbmm.lodz.pl).

Contract grant sponsor: Polish Ministry of Scientific Research and Information Technology; contract grant number: 3T08C00728.

Journal of Applied Polymer Science, Vol. 105, 122–129 (2007)
© 2007 Wiley Periodicals, Inc.

cal emission spectroscopy.²⁹ The film growth rate and deposition yield for $c_N = 0.88$ were found to be 4–5 times higher than those in the case of pure hydrogen or nitrogen being used as the plasma-generating upstream gas, that is, for $c_N = 0$ or 1.²⁹

In view of these data, the Si : C : N coatings were produced in this work with the N₂ content in the H₂–N₂ plasma-generating mixture being $c_N = 0.88$. The effect of the deposition (or substrate) temperature on the rate and yield of RP-CVD, as well as the chemical structure of the resulting coatings, is reported. The coatings were characterized in terms of their basic physical and mechanical properties, which are important for technological applications. In particular, the density (ρ), hardness (H), elastic modulus (E), and friction coefficient (μ) have been examined. The correlations between the chemical structure [controlled by the substrate temperature (T_S)] and the properties of the Si:C:N coatings have been determined. The presented structure–property relationships seem to be an important aspect for extending our knowledge of this useful class of coating materials.

EXPERIMENTAL

Film deposition procedure

The RP-CVD system used for the formation of Si:C:N films has been presented and described in detail elsewhere.²⁹ The apparatus consisted of the plasma-generation section fed with nitrogen and coupled to a 2.45-GHz microwave power supply unit, the remote section equipped with Wood's horn photon trap, and the CVD reactor fed with the precursor vapor and containing the substrate holder equipped with a heater. Deposition experiments were performed at a total flow rate of the upstream gas mixture of $F(\text{H}_2 + \text{N}_2) = 100$ sccm, c_N (0.88) being kept constant in the mixture; the total pressure was 85 Pa, and microwave power input was 120 W. The TMDSN precursor, the Pharmaceutical Chemical Reagents Inc. (PCR) product (Gainesville, FL), was evaporated at 20°C and fed into the CVD reactor at a flow rate of $F(\text{TMDSN}) = 1.7$ – 2.6 mg/min = 0.3–0.4 sccm. The distance between the plasma edge and the precursor inlet was 40 cm. No film deposition was observed in the plasma section, and this indicated that there was no back-diffusion of the precursor. The films were deposited on Fisher microscope cover-glass plates (45 × 50 × 0.2 mm) and on p-type crystalline silicon (c-Si) wafers (3 cm × 3 cm × 0.4 mm) at $T_S = 30$ – 400°C . As film deposition did not occur without the use of plasma, the contribution of the thermally induced CVD process could be excluded.

Film characterization techniques

The thickness of the films deposited onto the c-Si wafers was measured ellipsometrically with a Nippon

Infrared Industrial Co. (Tokyo, Japan) EL-101D ellipsometer equipped with a 632.8-nm He–Ne laser. For each film sample, the average thickness value was calculated from at least five ellipsometric measurements.

The reflection high-energy electron diffraction (RHEED) analyses of the films were performed with a JEM-100U (JEOL, Tokyo, Japan) electron microscope.

Fourier transform infrared (FTIR) absorption spectra of the films deposited onto c-Si wafers were recorded in a transmission mode on an FTIR Infinity ATI Matson (Madison, WI) spectrophotometer. The deconvolution of the FTIR absorption envelopes into individual absorption bands was performed with Gaussian functions for curve fitting.

ρ for the film was estimated from the independently determined mass of the deposit on cover-glass plates and thickness values, which were measured gravimetrically and ellipsometrically, respectively.

H and E data were determined from the nanoindentation measurements performed for approximately 0.8- μm -thick films deposited onto the p-type c-Si substrate with a Nano Test 600 instrument (Micro Materials Ltd., Wrexham, UK) equipped with a Berkovitch-type trigonal, pyramidal diamond indenter. Measurements were carried out at loads increasing from 0.05 to 4.2 mN at a constant rate of 0.45 mN/s. H and E were evaluated from the indentation data according to the method developed by Oliver and Pharr,³³ with software provided by the instrument manufacturer. To reduce the effect of the substrate material, the analyzed data were obtained for the case of penetration depths not exceeding 20% of the film thickness.

The friction force of a stainless steel ball with the radius of 5 μm sliding over the film surface was measured with the same instrument used for nanoindentation (i.e., the Nano Test 600) but now equipped with a friction attachment. Measurements were carried out for films deposited on the c-Si substrate, at a normal load of 8 mN and sliding speed of 100 nm/s, over the distance of 100 μm , in ambient air (temperature = 21–22°C, relative humidity = 44%). The topography of the scanned surfaces was registered along with the friction force to eliminate the influence of possible artifacts on the measurements.

RESULTS AND DISCUSSION

Film growth rate and growth yield

The RP-CVD process has been characterized by the determination of the thickness-based film growth rate (r_d) and film growth yield (k_d). The latter parameter is defined as $k_d = r_d/F$, where F denotes the mass-based precursor flow (or feeding) rate. In physical terms, parameter k_d expresses the thickness of the deposit per unit of mass of the precursor fed into the reactor.

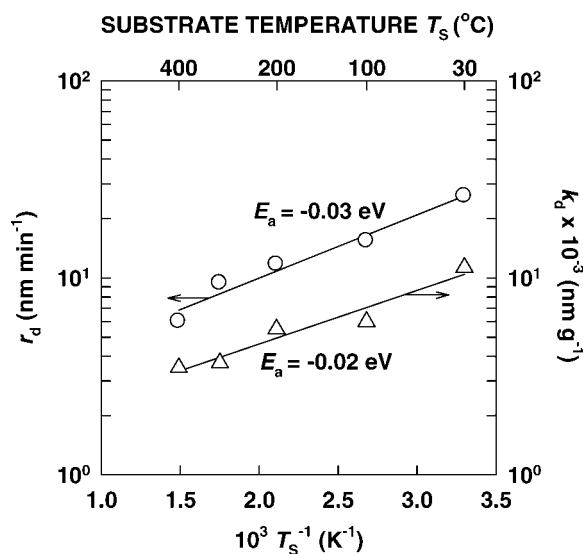


Figure 1 (○) r_d and (△) k_d of Si : C : N films as a function of the inverse of T_S .

Figure 1 shows the T_S dependence of r_d and k_d , determined in the form of Arrhenius plots. As can be noted from these plots, the values of r_d and k_d decrease with increasing T_S . The negative values of the apparent activation energy, $E_a = -0.03$ eV and $E_a = -0.02$ eV, resulting from the slopes of the r_d and k_d Arrhenius plots, respectively, imply that the RP-CVD is mainly controlled by the adsorption of film-forming precursors from the gas phase onto the growth surface. In this case, E_a is expressed as $E_a = E_r + \Delta E_{ad}$, where E_r denotes the activation energy of the film-forming reaction and ΔE_{ad} is the apparent heat of adsorption of the film-forming precursors and has a negative value.^{34,35} Thus, the negative E_a values are due to the fact that the absolute ΔE_a value is higher than the E_r value. These results account for the adsorption of the precursors onto the growth surface as the major factor limiting the film growth rate. It is worth mentioning that an analogous thermal activation effect, exhibiting $E_a < 0$, has been observed for RP-CVD³⁵ and DP-CVD^{36–40} involving a number of organosilicon precursors.

Film structure

The Si:C:N films deposited at different T_S values were examined in terms of their microstructure with RHEED analysis. The RHEED patterns obtained for the films deposited at different T_S values in the examined range of $T_S = 30$ – 400°C revealed the absence of reflexes that might be assigned to the crystalline structure, thus accounting for the amorphous structure of the films.

An FTIR spectroscopy examination of these Si : C : N films provided important information about the chemi-

cal bonds and groups contributing to the film bulk structure. Figure 2 shows the FTIR spectra of the Si:C:N films deposited at various T_S values. The particular absorption bands were identified with the literature data.^{41,42}

The film spectra in Figure 2 reveal the presence of the following absorption bands:

- The intense broad band in the range of 1400 – 700 cm^{-1} , including overlapped signals from the Si–Me deformation mode (1266 – 1263 cm^{-1}), N–H bending mode of Si–NH–Si and/or Si–NH–C (1188 – 1172 cm^{-1}), –CH₂– wagging mode of Si–CH₂–Si and/or Si–O asymmetric stretching mode (1039 – 1019 cm^{-1}), Si–N stretching mode (940 – 916 cm^{-1}), and Si–C stretching mode (846 – 798 cm^{-1}).
- The band in the range of 1720 – 1718 cm^{-1} [Fig. 2(a,b)] from the stretching mode of C=O.
- The band in the range of 2400 – 2000 cm^{-1} composed of two overlapped signals from the C≡N stretching mode of Si–CN (2196 – 2189 cm^{-1}) and Si–H stretching mode (2150 – 2101 cm^{-1}).
- Weak intensity bands in the range of 2973 – 2906 cm^{-1} [Fig. 2(a–c)] from the asymmetric stretching mode of C–H.
- The band in the range of 3368 – 3360 cm^{-1} from the stretching mode of N–H in the Si–NH–Si and/or Si–NH–C units.

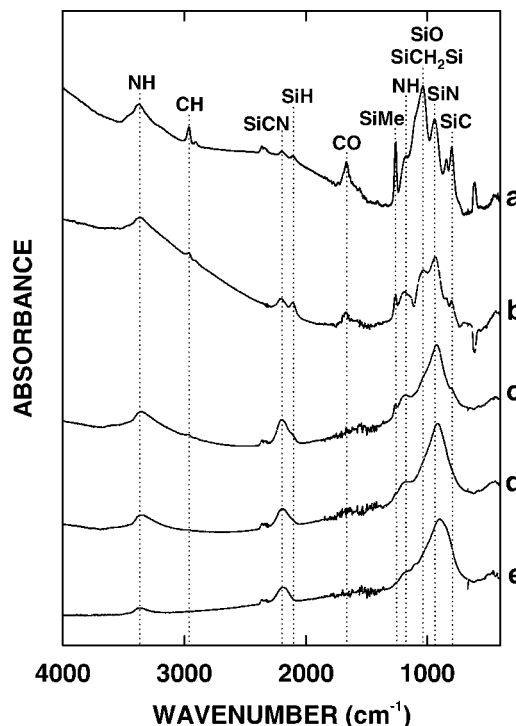


Figure 2 FTIR transmission spectra of Si : C : N films deposited on c-Si wafers at various deposition temperatures: (a) 30 , (b) 100 , (c) 200 , (d) 300 , and (e) 400°C .

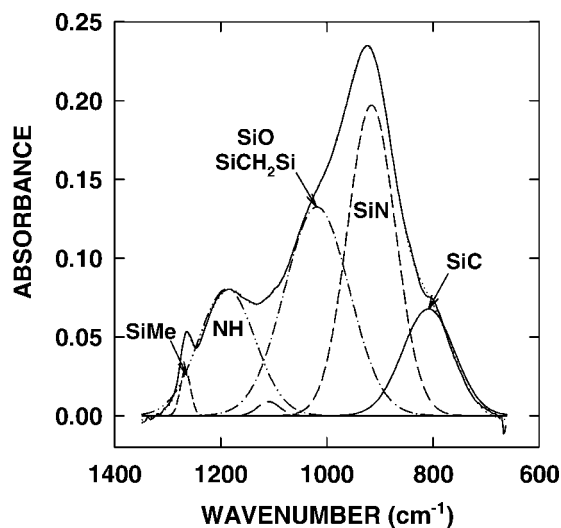


Figure 3 Example of a resolved IR absorption band in the range of $1350\text{--}650\text{ cm}^{-1}$ for a Si : C : N film deposited at $T_S = 200^\circ\text{C}$.

The increase in T_S involves marked changes to the film spectra, as revealed in Figure 2. To obtain quantitative information about the evolution of the film structure, the spectral envelope ranging from 1350 to 650 cm^{-1} (Fig. 2) has been resolved into the component bands. This resolution is exemplified in Figure 3 for the case of a film produced at $T_S = 200^\circ\text{C}$, showing component bands from the Si—Me (1266 cm^{-1}), N—H (1188 cm^{-1}), Si—CH₂—Si and/or Si—O (1019 cm^{-1}), Si—N (916 cm^{-1}), and Si—C (809 cm^{-1}) units. The band at 1019 cm^{-1} cannot be resolved into the Si—CH₂—Si and Si—O components because of their extremely strong overlap.

Oxygen contamination, revealed by the Si—O band contribution, may originate from two potential sources. The first may be the etching of the glass walls of the CVD system by highly reactive atomic species from the plasma, resulting in the incorporation of oxygen-containing etch products into the growing film.⁴³ The second source may arise from the reactions of long-lived dangling bonds in the deposit with atmospheric oxygen or moisture, which may occur after the film is exposed to the ambient environment.

The relative integrated intensities of the component Si—N, Si—C, N—H, and SiMe bands (determined as the ratio of the particular component band area to its envelope area) are shown in Figure 4 as a function of T_S . The IR intensity curves in Figure 4 reveal the following trends with increasing T_S :

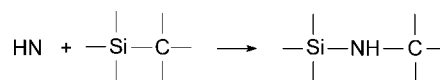
- The marked rise in the intensity of the Si—C band.
- The increase in the intensities of the Si—N and N—H bands to the maximum values at $T_S = 100^\circ\text{C}$ and drop for $100^\circ\text{C} < T_S \leq 400^\circ\text{C}$.

- The increase in the intensity of the Si—CH₂—Si and/or Si—O band to the maximum value at $T_S = 200^\circ\text{C}$ and decrease for $200^\circ\text{C} < T_S \leq 400^\circ\text{C}$.
- The decrease in the intensity of the SiMe band to nearly zero at $T_S = 300^\circ\text{C}$.

The IR data in Figure 4 account for the elimination of the methyl groups and thermally enhanced crosslinking leading to the formation of the Si:C:N network structure in the film deposited at a high T_S regime. However, the Si—C bonds appear to prevail over the Si—N bonds in the network.

Crosslinking reactions

On the basis of the results of the structural study, hypothetical mechanisms of some elementary reactions contributing to the crosslinking process in the Si:C:N film can be postulated. The rise in the intensities of the Si—N and N—H IR bands for $T_S \leq 100^\circ\text{C}$ (Fig. 4) may be ascribed to the insertion of hydronitrene into the Si—C bonds in the methylsilyl groups and into the segments of the film network, resulting in the formation of the Si—NH—C units. This process takes place at the growth surface via eq. (1).^{29,30}



The incorporation of hydronitrene species into the film according to eq. (1) lengthens the crosslinks and subsequently leads to loosening of the film network. Therefore, this process seems to markedly affect the Si : C : N film properties.

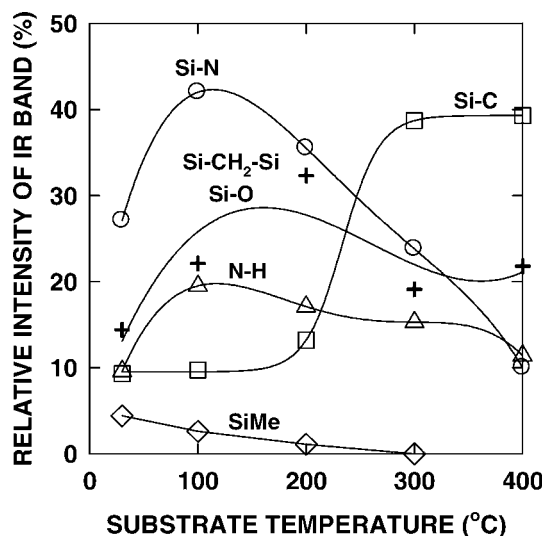
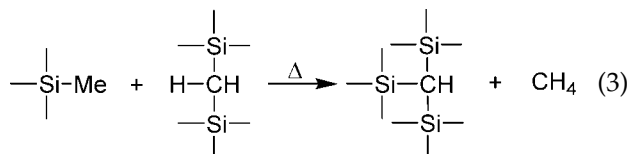
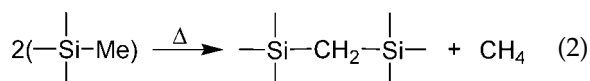


Figure 4 Relative integrated intensities of IR bands corresponding to the (○) Si—N, (□) Si—C, (△) N—H, (+) Si—CH₂—Si/Si—O, and (◇) SiMe units in an Si:C:N film as a function of T_S .

The marked rise in the intensity of the Si—C IR band observed with increasing T_S in Figure 4 is due to thermally enhanced crosslinking reactions involving the methylsilyl groups, which, according to the chemistry of pyrolysis of poly(methylcarbosilanes),^{44–47} may proceed via eqs. (2) and (3):



The formation of carbosilane crosslinks via eq. (2) is in agreement with the maximum appearing in the Si—CH₂—Si/Si—O intensity curve (Fig. 4). Equations (2) and (3) well explain the elimination of the methylsilyl groups revealed by the IR intensity SiMe curve in Figure 4.

Structure–property relationships

The relative integrated IR absorption intensity data in Figure 4 were used for determining the relationships between the Si:C:N film structure and its physical and mechanical properties.

ρ

ρ for the film, an important physical property strongly sensitive to crosslinking, is shown in Figure 5 as a function of the relative intensities of the IR absorption bands from the Si—N, N—H, and Si—C bonds, controlled by T_S . From the plots in Figure 5(a,b), it can be inferred that increasing contents of the Si—N and N—H bonds in the film cause a signifi-

cant drop of the ρ value from 3 to 1.7 g/cm³. This is due to the earlier mentioned loosening of the film network resulting from the formation of Si—NH—C bonds via eq. (1). On the other hand, the increase in the content of the Si—C bonds in the film network gives rise to the ρ value [Fig. 5(c)]. This strong densification of the film can be ascribed to thermally induced crosslinking reactions expressed by eqs. (2) and (3).

The high ρ value (3.0 g/cm³) of the Si:C:N film deposited at $T_S = 400^\circ\text{C}$ (Fig. 5) is close to those of crystalline silicon nitride ($\rho = 3.2 \text{ g/cm}^3$)⁴⁸ and silicon carbide ($\rho = 3.1 \text{ g/cm}^3$).⁴⁹ For comparison, the ρ values reported for Si : C : N films produced by DP-CVD from the mixtures of hexamethyldisilazane and hydrogen⁶ at $T_S = 350^\circ\text{C}$ and diethylsilane and ammonia⁵⁰ at $T_S = 300^\circ\text{C}$ are 2.3 and 2.1 g/cm³, respectively.

H and E

Figure 6 shows the plots of H and E as functions of the relative integrated intensities of the IR bands from the Si—N, N—H, and Si—C bonds, controlled by T_S . The plots indicate that H and E vary in the ranges of $H = 2.5\text{--}16.2 \text{ GPa}$ and $E = 43\text{--}187 \text{ GPa}$ (for $T_S = 100\text{--}400^\circ\text{C}$). H and E , determined for the c-Si substrate, are 12 and 199 GPa, respectively.

It can be inferred from the presented plots that the H and E values decrease markedly with increasing contents of the Si—N and N—H bonds [Fig. 6(a,b), respectively] and increase with rising contents of the Si—C bonds [Fig. 6(c)]. It is interesting to note that the trends in the H and E plots in Figure 6(a–c) are similar to those in respective ρ plots in Figure 5(a–c). This accounts for the reasonably good correlation existing between H and E of the film and its ρ . Thus, the drop in the H and E values in Figure 6(a,b) is evidently due to the decreasing ρ value of the film, as

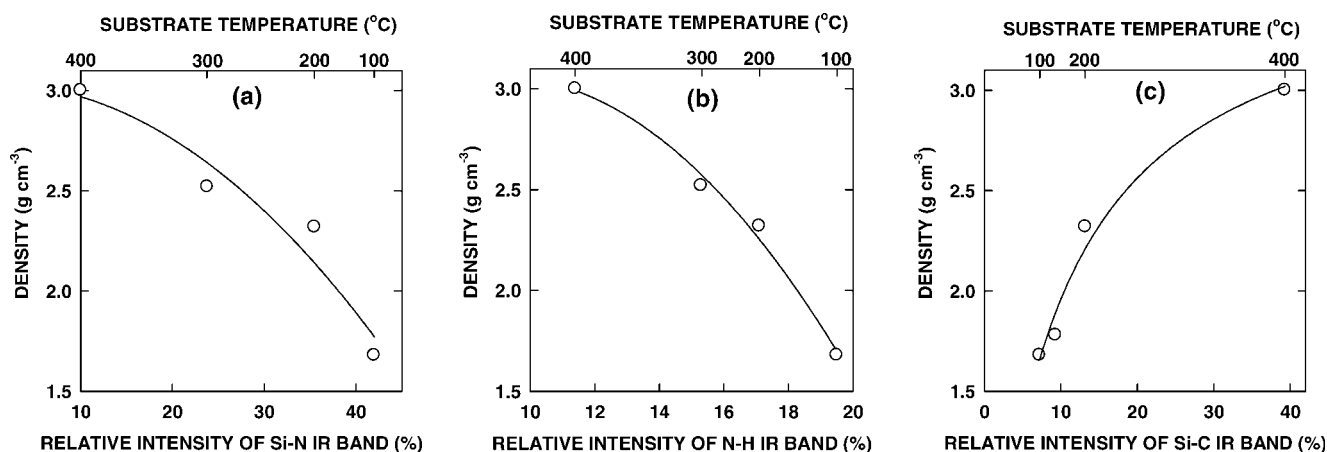


Figure 5 ρ of Si:C:N films as a function of the relative integrated intensities of IR absorption bands from (a) Si—N, (b) N—H, and (c) Si—C bonds, controlled by T_S .

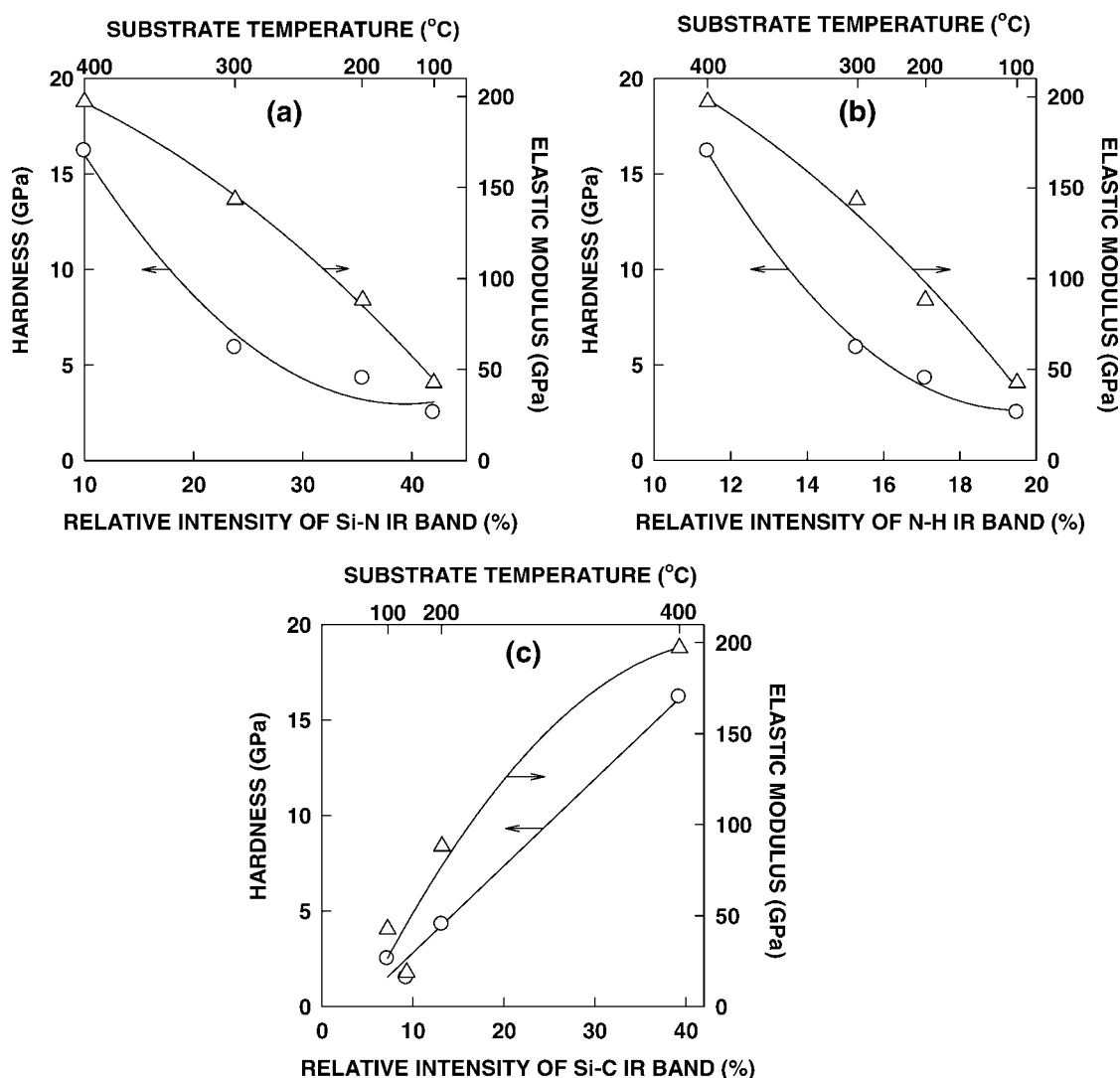


Figure 6 (○) H and (△) E of SiC:N films deposited onto c-Si substrates as a function of the relative integrated intensities of the IR absorption bands from (a) Si–N, (b) N–H, and (c) Si–C bonds, controlled by T_S .

shown in Figure 5(a,b), whereas their increase in Figure 6(c) can be ascribed to densification of the film resulting from the rising content of the Si–C cross-links, as can be inferred from Figure 5(c).

For comparison with the H and E values for these films, the literature data on Si : C : N films formed on a c-Si substrate by DP-CVD from hexamethyldisilazane at $T_S = 300\text{--}450^\circ\text{C}$,⁹ from diethylsilane and ammonia at $T_S = 100\text{--}300^\circ\text{C}$,⁵⁰ from silane, methane, and nitrogen,¹⁰ and from silane, ethylene, and nitrogen at $T_S = 400^\circ\text{C}$ ⁵¹ revealed $H = 12\text{--}18$ GPa,⁹ $H = 1\text{--}13$ GPa and $E = 40\text{--}100$ GPa,⁵⁰ $H = 24\text{--}33$ GPa and $E = 150\text{--}198$ GPa,¹⁰ and $H = 11\text{--}13$ GPa,⁵¹ respectively.

μ

Figure 7 shows the effects of structural parameters expressed by the relative integrated intensities of the IR absorption bands from the Si–N and Si–C bonds, controlled by T_S , on μ of the a-Si : C : N : H film. The

presented structural plots indicate that μ varies in a narrow range of small values ($\mu = 0.02\text{--}0.05$). For comparison, μ measured for the c-Si substrate was 0.07. It can be inferred from the presented plots that μ decreases with an increasing content of the Si–N bonds [Fig. 7(a)] and rises slightly with an increasing content of the Si–C bonds [Fig. 7(b)].

With the same technique used in this study, we have measured the μ values for silicon carbide (a-Si:C:H) films deposited on c-Si at $T_S = 100\text{--}300^\circ\text{C}$ by RP-CVD from tetramethyldisilazane and (dimethylsilyl)(trimethylsilyl)methane precursors with hydrogen as a plasma-generating upstream gas.⁵² The reported μ values were in the range of 0.04–0.05.⁵²

CONCLUSIONS

The negative values of E_a resulting from the slopes of the thermal activation plots of the film growth rate

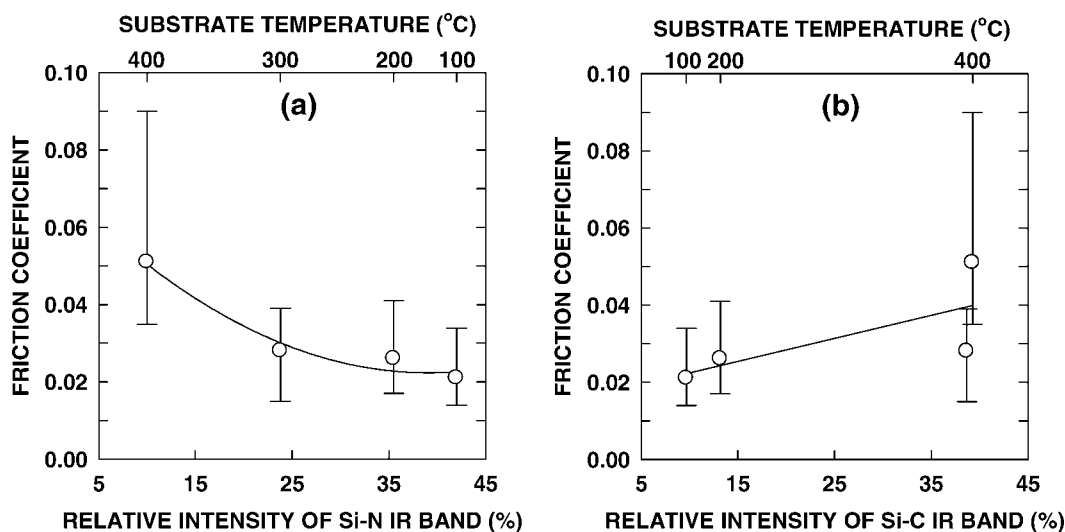


Figure 7 μ (against stainless steel) of Si : C : N films deposited onto c-Si substrates as a function of the relative integrated intensities of the IR absorption bands from (a) Si—N and (b) Si—C, controlled by T_S .

and film growth yield imply that the investigated RP-CVD process is controlled by the adsorption of film-forming precursors from the gas phase onto the growth surface.

As revealed by the results of the IR study, T_S is a key parameter strongly influencing the chemical structure of the Si : C : N films. An increase in T_S leads to the elimination of the organic groups and subsequent crosslinking via the formation of the Si—C and Si—N networks. However, in a high T_S range (300–400°C), the formation of the Si—C crosslinks dominates.

Distinct relationships were found to exist between the IR structural parameters, related to the Si—N and Si—C bonds and the NH units (in Si—NH—Si and/or Si—NH—C crosslinks), and the Si : C : N film properties, such as ρ , H , and E . An increase in the contents of the Si—N and N—H bonds was found to accompany significant drops in ρ , H , and E . Opposite trends were observed for the case of Si—C bonds: ρ , H , and E were found to increase markedly with rising contents of Si—C bonds in the film network. μ varied in a very narrow range of small values ($\mu = 0.02$ – 0.05) and dropped with increasing contents of the Si—N bonds. The increase in the contents of the Si—C bonds caused a slight rise in μ .

In view of the relatively high H value (16 GPa) and low μ value (0.05 against stainless steel) found for the a-Si : C : N film deposited at $T_S = 400^\circ\text{C}$, this material may be useful as a tribological coating for metals.

The authors thank D. Bielinski (Technical University of Lodz) for his kind assistance with the indentation measurements.

References

- Heyner, R.; Marx, G. *Thin Solid Films* 1995, 258, 14.
- He, Z.; Carter, G.; Colligon, J. S. *Thin Solid Films* 1996, 283, 90.
- Kim, M. T.; Lee, J. *Thin Solid Films* 1997, 303, 173.
- Scharf, T. W.; Deng, H.; Barnard, J. A. *J Vac Sci Technol A* 1997, 15, 63.
- Bendeddouche, A.; Bejoran, R.; Beche, E.; Hillel, R. *Surf Coat Technol* 1999, 111, 184.
- Marx, G.; Korner, K. U.; Hager, P. *Steel Res* 2001, 72, 518.
- Berlind, T.; Hellgren, N.; Johansson, M. P.; Hultman, L. *Surf Coat Technol* 2001, 141, 145.
- Vlcek, J.; Kormunda, M.; Cizek, J.; Perina, V.; Zemek, J. *Surf Coat Technol* 2002, 160, 74.
- Kuo, D. H.; Yang, D. G. *Thin Solid Films* 2000, 374, 92.
- Jedrzejowski, P.; Cizek, J.; Amassian, A.; Klemberg-Sapieha, J. E.; Vlcek, J.; Martinu, L. *Thin Solid Films* 2004, 447–448, 201.
- Sarang, D.; Sanjines, R.; Karimi, A. *Thin Solid Films* 2004, 447–448, 217.
- Probst, D.; Hoche, H.; Zhou, Y.; Hauser, R.; Stelzner, T.; Scheerer, H.; Broszeit, E.; Berger, C.; Riedel, R.; Stafast, H.; Koke, E.; *Surf Coat Technol* 2005, 200, 355.
- Vetter, M.; Martin, I.; Orpella, A.; Puigdollers, J.; Voz, C.; Alcu-billa, R. *Thin Solid Films* 2004, 451–452, 340.
- Zhang, D. H.; Gao, Y.; Wei, J.; Mo, Z. Q. *Thin Solid Films* 2000, 377–378, 607.
- Yasui, K.; Nasu, M.; Komaki, K.; Kaneda, S. *Jpn J Appl Phys* 1990, 29, 918.
- Tarntair, F. G.; Wu, J. J.; Chen, K. H.; Wen, C. Y.; Chen, L. C.; Cheng, H. C. *Surf Coat Technol* 2001, 137, 152.
- Wu, J. Y.; Kuo, C. T.; Liu, T. L. *Thin Solid Films* 2001, 398–399, 413.
- Lin, H. Y.; Chen, Y. C.; Lin, C. Y.; Tong, Y. P.; Hwa, L. G.; Chen, K. H.; Chen, L. C. *Thin Solid Films* 2002, 416, 85.
- Riedel, R.; Kleebe, H.; Schonfelder, H.; Aldinger, F. *Nature* 1995, 374, 526.
- Badzian, A.; Badzian, T.; Drawl, W. D.; Roy, R. *Diamond Relat Mater* 1998, 7, 1519.
- Bae, Y. B.; Du, H.; Gallois, B.; Gonsalves, K. E.; Wilkens, B. J. *Chem Mater* 1992, 4, 478.
- Matsutani, T.; Asanuma, T.; Liu, C.; Kiuchi, M.; Takeuchi, T. *Surf Coat Technol* 2003, 169–170, 624.

23. Di Mundo, R.; d'Agostino, R.; Fracassi, F.; Palumbo, F.; Plasma Process Polym 2005, 2, 612.
24. Smirnova, T. P.; Badalyan, A. M.; Borisov, V. O.; Yakovkina, L. V.; Kaichev, V. V.; Shmakov, A. N.; Nartova, A. V.; Rakhlin, V. I.; Fomina, A. N. J. Struct Chem 2003, 44, 169.
25. Fainer, N. I.; Rumyantsev, Y. M.; Kosinova, M. L.; Yurjev, G. S.; Maximovski, E. A.; Kuznetsov, F. A. Appl Surf Sci 1997, 114, 614.
26. Fainer, N. I.; Kosinova, M. L.; Rumyantsev, Y. M.; Kuznetsov, F. A. J Phys IV 1999, 9, 769.
27. Kosinova, M. L.; Fainer, N. I.; Rumyantsev, Y. M.; Terauchi, M.; Shibata, K.; Satoh, F.; Kuznetsov, F. A. J Phys IV 2001, 11, 987.
28. Fainer, N. I.; Rumyantsev, Y. M.; Golubenko, A. N.; Kosinova, M. L.; Kuznetsov, F. A. J. Cryst Growth 2003, 248, 175.
29. Wrobel, A. M.; Blaszczyk, I.; Walkiewicz-Pietrzykowska, A.; Tracz, A.; Klemberg-Sapieha, J. E.; Aoki, T.; Hatanaka, Y. J Mater Chem 2003, 13, 731.
30. Wrobel, A. M.; Blaszczyk-Lezak, I.; Walkiewicz-Pietrzykowska, A.; Bieliński, D. M.; Aoki, T.; Hatanaka, Y. J Electrochem Soc C 2004, 151, 723.
31. Blaszczyk-Lezak, I.; Wrobel, A. M.; Kivitorma, M. P. M.; Vayrynen, I. J Chem Vap Deposition 2005, 11, 44.
32. Aoki, T.; Ogishima, T.; Wrobel, A. M.; Nakanishi, Y.; Hatanaka, Y. Vacuum 1998, 51, 747.
33. Oliver, W. C.; Pharr, G. M. J Mater Res 1992, 7, 1564.
34. Raupp, G. B.; Shemansky, F. A.; Cale, T. S. J Vac Sci Technol B 1992, 10, 2422.
35. Wrobel, A. M.; Walkiewicz-Pietrzykowska, A.; Wickramanayaka, S.; Hatanaka, Y. J Electrochem Soc 1998, 145, 2867.
36. Secrist, D. R.; Mackenzie, J. D. J Electrochem Soc 1966, 113, 914.
37. Emesh, I. T.; d'Asti, G.; Mercier, J. S.; Leung, P. J Electrochem Soc 1989, 136, 3404.
38. Wrobel, A. M.; Kryszewski, M. Prog Colloid Polym Sci 1991, 85, 91.
39. Favia, P.; Lamendola, R.; d'Agostino, R. Plasma Sources Sci Technol 1992, 1, 59.
40. Niemann, J.; Bauhofer, W. Thin Solid Films 1999, 352, 249.
41. Anderson, D. R. In Analysis of Silicones; Smith, A. L., Ed.; Wiley-Interscience: New York, 1974; Chapter 10.
42. Sokrates, G. Infrared Characteristics Group Frequencies; Wiley-Interscience: Chichester, England, 1994; Chapter 18.
43. Wrobel, A. M.; Wickramanayaka, S.; Nakanishi, Y.; Fukuda, Y.; Hatanaka, Y. Chem Mater 1995, 7, 1403.
44. Yajima, S.; Hasegawa, Y.; Hayashi, J.; Imura, M. J Mater Sci 1978, 13, 2569.
45. Hasegawa, Y.; Okamura, K. J Mater Sci 1983, 18, 3633.
46. Birot, M.; Pillot, J. P.; Dunogues, J. Chem Rev 1995, 95, 1443.
47. Laine, R. M.; Babonneau, F. Chem Mater 1993, 5, 260.
48. Riedel, R. Adv Mater 1994, 6, 549.
49. Plano, L.; Pinneo, M. In Diamond Films and Coatings; Davies, R. F., Ed.; Noyes: Park Ridge, NJ, 1993; Chapter 7.
50. Levy, R. A.; Chen, L.; Grow, J. M.; Yu, Y. Mater Lett 2002, 54, 102.
51. Afanasyev-Charkin, I. V.; Nastasi, M. Surf Coat Technol 2004, 186, 108.
52. Wrobel, A. M.; Walkiewicz-Pietrzykowska, A.; Bieliński, D. M.; Klemberg-Sapieha, J. E.; Nakanishi, Y.; Aoki, T.; Hatanaka, Y. Chem Mater 2003, 15, 1757.